Predicting Lithium-ion Battery Resistance Degradation using a Log-Linear Model

Vilsen, Søren Byg; Kær, Søren Knudsen; Stroe, Daniel-Ioan

Published in:
Proceedings of 2019 IEEE Energy Conversion Congress and Exposition (ECCE)

DOI (link to publication from Publisher):
10.1109/ECCE.2019.8912770

Publication date:
2019

Document Version
Accepted author manuscript, peer reviewed version

Predicting Lithium-ion Battery Resistance Degradation using a Log-Linear Model

1st Søren B. Vilsen
Department of Energy Technology and Department of Mathematical Sciences
Aalborg University
Aalborg, Denmark
svilsen@math.aau.dk

2nd Søren Knudsen Kaer
Department of Energy Technology
Aalborg University
Aalborg, Denmark
skk@et.aau.dk

3rd Daniel-Ioan Stroe
Department of Energy Technology
Aalborg University
Aalborg, Denmark
dis@et.aau.dk

***Abstract*—The resistance is one of the parameters that describes the performance of Lithium-ion (Li-ion) batteries, as it offers information about the battery efficiency and its power capability. However, similar to other performance parameters of Li-ion batteries, the resistance is dependent on the operating conditions and increases while the battery is aging. Traditionally, to capture these dependencies, Li-ion cells are aged at different conditions using synthetic mission profiles and periodically the aging tests are stopped in order to measure the resistance at standard conditions. Most of the times, even though accurate information about the resistance behavior is obtained, they do not reflect the behavior from real-life applications. Thus, in this work we propose a method for extracting, modelling, and predicting the resistance directly from the battery dynamic mission profile. While the extraction mainly relied on data manipulation and bookkeeping, the modelling and subsequent prediction of the resistance used a log-linear model.**

***Index Terms*—Lithium-ion battery, Resistance estimation, Battery Degradation, Dynamic aging profile, Log-linear model**

I. Introduction

The internal resistance, together with the capacity, is one of the parameters, which describes the performance and lifetime behavior of Lithium-ion (Li-ion) batteries [1]. The internal resistance is used to determine the power capability of batteries [2], which is an important parameter in both renewable energy storage applications and electric vehicle (EV) applications. Thus, by having accurate knowledge about the internal resistance, and subsequently, on the power capability, battery systems can be optimally sized in order to meet both the technical and economic requirements of a certain application. Furthermore, the internal resistance is an important parameter for battery electrical and thermal modeling, as it describes the dynamic and heat generation behavior of the battery, respectively [3], [4].

The internal resistance of Li-ion batteries is a very nonlinear parameter, which is changing depending on the operating temperature, load current, and on the battery state-of-charge (SOC) [3], [8]. Moreover, the internal resistance of the battery is age-dependent, increasing in time during long-term operation [5], [14]. Different methods for determining the internal resistance of the Li-ion batteries exist [6]. However, most of the time, the internal resistance is determined using the current pulse technique, where a charging/discharging current of a certain amplitude and length is applied to the battery and the voltage response of the battery is registered [2], [5]. Then, the internal resistance is calculated using Ohms Law. This method is successfully applied in laboratory conditions, in order to determine the internal resistance of the battery at different conditions and to track the changes of the internal resistance during battery aging [5]. Nevertheless, a major drawback of this method is represented by the fact that before the resistance measurement, the battery has to be in idling mode, for a certain amount of time (i.e., at least 15 minutes), in order to reach thermo-dynamic stability. Consequently, this requirement makes the method less suitable for real-life applications, where downtime periods of the Li-ion storage system is not technical and economic feasible.

As aforementioned, if it is possible to perform reference measurements during the aging of the battery, then the effects of aging on the internal resistance can be easily estimated using e.g. a power law function as illustrated in [9], [10]. However, identification of the internal resistance and estimation of the subsequent degradation from a dynamic real-life aging profile requires more sophisticated methods. In recent years an explosion of various online-estimation methods have been introduced, such as the many Kalman-filter variants [11], [12] combined with either an additional filter or a recursive estimation procedure. There are also notable exceptions like the series resistance determination (SRD) algorithm combined with an exponential moving average [13].

In this paper, the feasibility of tracking the degradation of the internal resistance directly from a real-life mission profile, which is used to age the battery over a period of 38 weeks, was analysed. The internal resistance is extracted, in a similar fashion to the idea behind the SRD algorithm [13], by keeping careful track of the beginning and length of current pulses. The logarithm of the extracted resistance was assumed to follow a normal distribution, where the mean was a non-linear function of the battery's SOC. The parameters of the internal resistance model were estimated on a week-by-week basis, allowing for the tracking of the changes to the resistance over time. Using the estimated parameters and making assumptions

about the prior probability of the SOC and week values, the exact distribution of the battery's age given a new internal resistance value and the SOC at which this was measured can be calculated using Bayes rule [7] and the law of total probability [7]. Finally, the results, obtained with the proposed method are compared with results obtained from resistance measurement using the traditional method, which were carried out after each week of battery aging.

II. Experiment

A. Lithium-ion battery under test

In this work a cylindrical Li-ion battery cell with a nominal capacity of 2.5 Ah and a nominal voltage of 3.3 V was used. The cell is based on a graphite anode and a lithium iron phosphate (LFP) cathode and it was designed for high power application being able to be continuously charged and discharged with current up to four times the nominal current.

B. Aging condition and internal resistance measurement

The Li-ion battery was aged using the current profile presented in Fig. 1, which has a length of one week. Furthermore, a particularity of the current profile is represented by the fact that in more than 95% of the occurrences a 4C-rate (i.e., 10 A) current was applied for both charging/discharging. When applied to the tested battery cell, the current profile resulted into the battery SOC profile, presented in Fig. 2, which varies in the interval 10% - 90% SOC. The aging profile presented in Fig. 1, was applied for a period of 38 weeks considering an aging temperature of 25^{o}C. For more details about the aging profile, the reader is referred to [15].

After each week of aging tests, the resistance of the battery was determined using the current pulse technique; the measurements were carried out at 20%, 50% and 80% SOC, considering a current pulse of 4C-rate (i.e., 10 A), which was applied for a length of 18 seconds. Before the current pulse was applied, the battery was in idling mode for 15 minutes, in order to reach thermo-dynamic stability. The obtained increase of the battery resistance during the 38 weeks of cycling is presented in Fig. 3. As one can observe, for the considered aging period, the resistance has increased only by 8.7%, even though the battery cell's capacity decreased by more than 15% in comparison to the value measured at the beginning of life, as it is presented in Fig. 4.

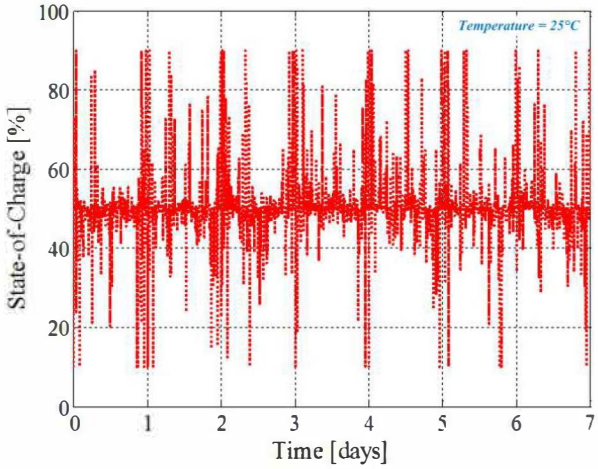

Fig. 2. The battery cell's SOC profile corresponding to one week of aging.

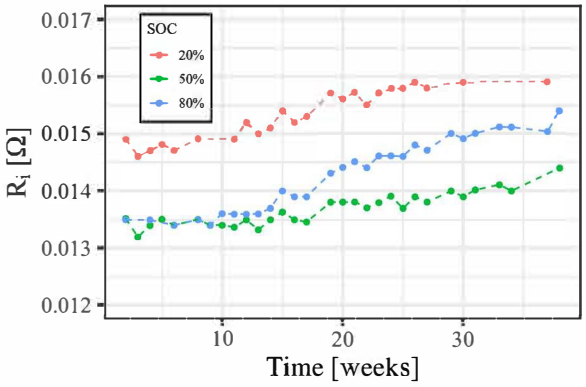

Fig. 3. The internal resistance increase during the aging test.

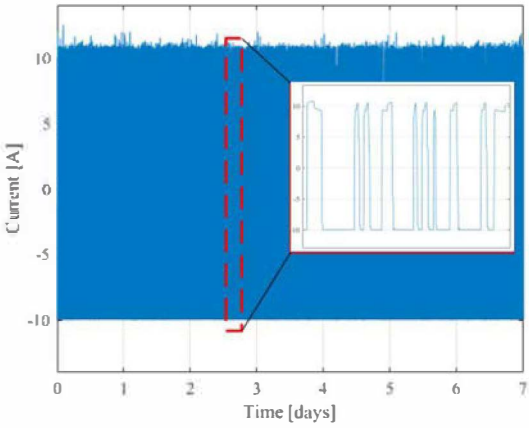

Fig. 1. One-week current profile used for aging the LFP-based Li-ion battery

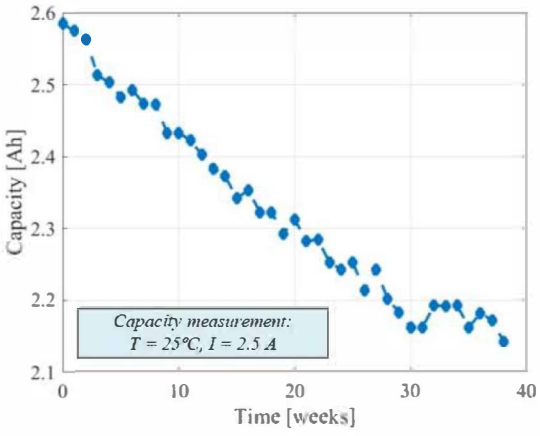

Fig. 4. The capacity fade behavior of the battery cell during the aging test.

III. Methodology

Extracting the internal resistance of the battery from a dynamic profile, as the one presented in Fig. 1, requires keeping track of the current, I, and of the voltage right before the beginning of the current pulse, V_s. If the current and voltage at a time t, and V_s, were given in advance, one could easily calculate the resistance at time t by Ohm's law, Eq. (1), for any given point along a current pulse (i.e. as long as $I_t \neq 0$).

$$R_{i,t} = \left| \frac{V_t - V_s}{I_t} \right| \tag{1}$$

Thus, what remains to be determined is when and how to update V_s. Focusing on the changes of the current from one point in time t, to the next point, $t+1$, the three following situations can be distinguished:

(1) The current changes from zero (i.e., the battery is idling) to a non-zero value (i.e., the battery is either charging or discharging).
(2) The current changes from one non-zero value to another non-zero value.
(3) The current does not change, i.e. the value at time t and $t+1$ are equivalent (within some small difference δ).

In the following, a brief description of the procedure for updating V_s on each of the three aforementioned situations will be given.

A. Situation in item (1)

In the first situation, V_s is updated using the voltage of the last instance when the current was zero (i.e. if $|I_t| < \varepsilon$, and $|I_{t+1}| > \varepsilon$), thus, V_s will be equal to V_t. This approach is dependent on the relaxation time between the current pulses, for the battery voltage to reach (or at least get close to) the open circuit voltage (OCV) , i.e. ideally the current profile is shaped as in Fig. 5. The longer the relaxation time between pulses, the more accurate the estimation of the battery resistance.

B. Situation in item (2)

The second case is more complex, but a potential solution will be outlined in the followings. If the time since the battery was idling (i.e. there was no current flowing through the battery) is relatively short (should be optimised), then the currently stored V_s value should be accurate enough for determining the battery resistance. However, the longer the time since the last idling period, the more inaccurate this value is going to be, as sketch in Fig. 6. However, in order to get a model which is as accurate as possible, resistances extracted in this case will be ignored in the remainder of this paper. That is, only the cases where V_s was updated when no current was flowing through the battery were considered. With that said, two possible solutions to this problem could be:

(1) Instead of considering the change in the current from zero, we could consider the change in current from its present value. Consequently, the second situation reverts to the first situation, as seen in Fig. 5. That is, if $|I_t - I_{t-1}| < \varepsilon$, and $|I_{t+1} - I_t| > \varepsilon$, then we set $V_s = V_t$.
(2) If the battery SOC is known and a model of the relationship between the OCV and SOC is available, then the accuracy of the internal resistance estimation can easily be increased using this relationship to update V_s.

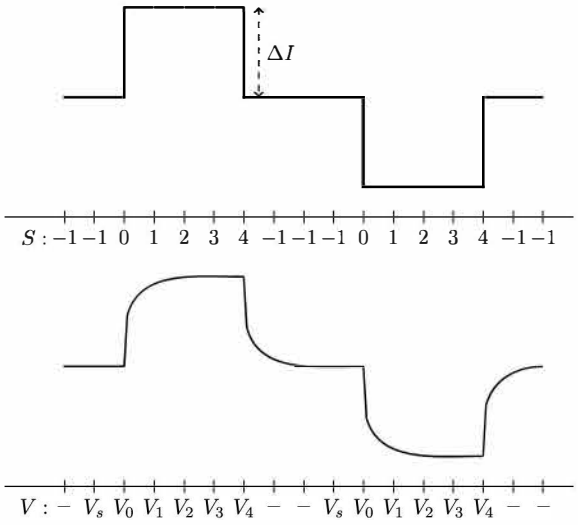

Fig. 5. A simple sketch of the two current pulses with a period of relaxation between pulses (top), and the resulting voltage (bottom).

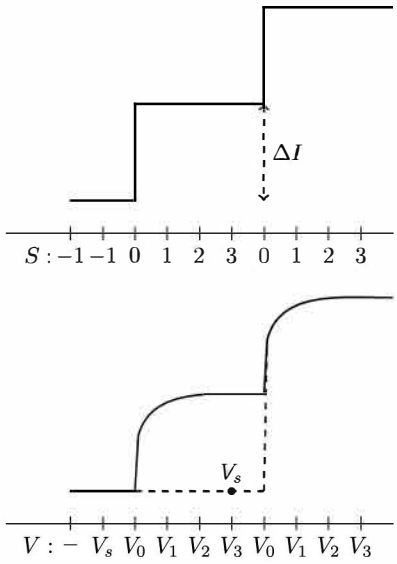

Fig. 6. A simple sketch of the current jumping from one C-rate of ΔI to $2\Delta I$ amperes, with no relaxation between the two C-rates (top), and the resulting voltage (bottom).

C. Situation in item (3)

In the third case, if the current does not change from time t to $t+1$, i.e. $|I_t - I_{t+1}| \leq \delta$, then V_s does not have to be updated. Therefore, we calculate the resistance at time $t+1$ using (1), and move on to the next iteration.

D. Relaxation period

The internal resistance is largely dependent on the length of the current pulse, as it is presented in [8]. Furthermore, after the current has been interrupted, it takes time for the battery to reach thermo-dynamic stability. Therefore, it is useful to also track the length of the previous pulse, L, and the length of any previous relaxation period T. Thus, it may be beneficial to restrict ourselves to resistances, which had longer relaxation times before updating V_s such that the voltage has time to stabilise. The effect of the relaxation period on the performance of the extraction method was investigated by comparing the results of (1) resistance identification requiring that the relaxation period has to be at least as long as the previous current pulse (i.e. where $T \geq L$), and (2) resistance identification requiring only one second of relaxation (i.e. where $T \geq 1$). The internal resistance extracted in the two cases will be denoted as R_i and $\tilde{R}_i$, respectively.

E. The characteristics of the estimated internal resistance

As the internal resistance was measured after each week of aging using a pulse length of 18 seconds, then the internal resistance extracted using the proposed methodology was defined as the resistance value after 18 seconds, i.e. $R_i = R_{i,18s}$. Furthermore, the considered dynamic aging profile, presented in Fig. 1, is characterized by many changes of the current all of the same C-rate amplitude. Thus, the internal resistance of the battery was estimated only for current values in the interval 9.5 A – 10.5 A, which allowed for (1) the insulation the dependence of the internal resistance on the current, and (2) an unbiased validation of the proposed method.

IV. Results

A. Internal resistance variation with SOC

Insulating the effects of the temperature, current (i.e., C-rate), and pulse length, the internal resistance of the tested battery cell, varies only with the SOC and increases while the battery is aging.

Based on previous studies [3], [8], it is well known that the internal resistance of the battery increases when approaching very low and very high SOCs. Thus, the dependence of the internal resistance on the SOC was expressed using:

$$R_i(\text{SOC}) = a \cdot \text{SOC}^b (1 - \text{SOC})^c, \tag{2}$$

where SOC takes values between 0 (fully discharged battery) and 1 (fully charged battery), and $a > 0$, while $b, c \leq 0$. Furthermore, considering the logarithm of (2), the relationship becomes linear in the parameter space, which is highly desirable for parameter estimation. Therefore, it is assumed that the logarithm of the battery resistance for a given week w, is:

$$\begin{aligned} \log(R_i) = \beta_{0,w} + \beta_{1,w} \cdot \log(\text{SOC}) \\ + \beta_{2,w} \cdot \log(1 - \text{SOC}) + \varepsilon, \end{aligned} \tag{3}$$

where ε follows a normal distribution with mean zero variance σ^2. Furthermore, it is assumed that the variance does not change from week-to-week. The parameters in (3) are estimated by maximum likelihood [7] under the assumption that $\beta_{1,w}$ and $\beta_{2,w}$ are both smaller than, or equal to, 0.

The internal resistance values extracted based on the considered aging profile and using the methodology presented in the previous section are illustrated in Fig. 7 and Fig. 8, for three different degradation levels of the battery cell. The results presented in Fig. 7 were obtained requiring a relaxation period T equal to the length of the previous current pulse, while the results presented in Fig. 8 were obtained requiring a relaxation period T equal to one second.

The internal resistance values estimated using the proposed methodology (black dots in Fig. 7 and Fig. 8) have been fitted using the model (2), where the blue line is the exponential of the expected log-resistance and the shaded area represents the 95% confidence interval. Furthermore, the red dots and the red dashed lines represent the internal resistance values extracted from the weekly check-ups and the model fitted to the extracted resistances at that corresponding month, respectively.

Comparing the results obtained for the two considered relaxation periods, it can be observed that while the number of internal resistance values is reduced by more than half, when imposing a stricter relaxation period requirement, the variation is also drastically reduced. In order to verify the accuracy of the proposed methodology for extracting the battery internal resistance from a dynamic mission profile, the absolute percentage error (APE) was calculated for every week of aging using:

$$\text{APE} = \left| \frac{y - \hat{y}}{y} \right|, \tag{4}$$

where y represents the internal resistance obtained during the weekly check-ups at the end of the aging period and $\hat{y}$ represents the internal resistance extracted from the dynamic profile using the proposed methodology. The values of the median APE for the 38 weeks are shown for both considered relaxation periods in Fig. 9 and Fig. 10, respectively. By comparing the obtained median APE's for the two relaxation periods, one can observe that the added restriction on the relaxation period, yields smaller median APE, as expected due to the smaller variance.

Furthermore, it has to be highlighted that the median APE presented in Fig. 9 is smaller than 4.5% in all but three cases. These results strongly suggest that the proposed internal resistance identification method can be used as an alternative approach for the traditional method, which needs the battery to be on stand-by for at least 15 minutes before the resistance measurement.

Fig. 11 shows the change in the estimated parameters of the log-linear resistance model over time. The figure shows that over time the β parameters decrease, while the standard

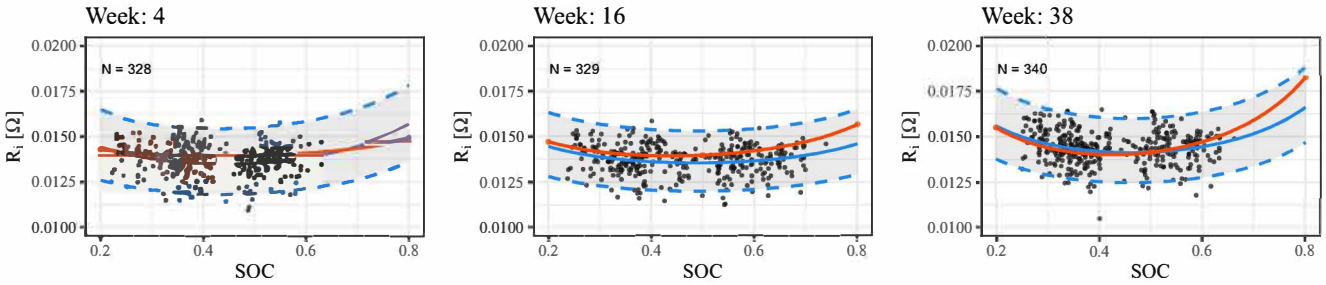

Fig. 7. Comparison between the internal resistance obtained during the periodic check-ups (traditional approach) and the internal resistance extracted from the dynamic profiles (investigated approach), at three different ageing levels: 4 weeks (left), 16 weeks (center), 38 weeks (right). The internal resistance was obtained considering a relaxation period at least as long as the previous current pulse.

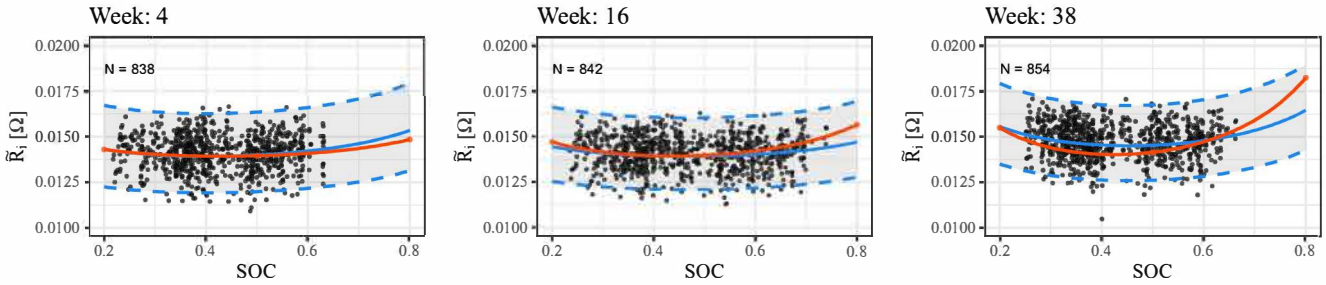

Fig. 8. Comparison between the internal resistance obtained during the periodic check-ups (traditional approach) and the internal resistance extracted from the dynamic profiles (investigated approach), at three different ageing levels: 4 weeks (left), 16 weeks (center), 38 weeks (right). The internal resistance was obtained considering a relaxation period of 1 second from the previous current pulse.

deviation of the model decreases in the beginning, but starts to increase towards the end. The decrease in $\beta_{1,w}$ and $\beta_{2,w}$ results in an increased (expected) internal resistance towards the edges of the SOC domain (i.e. close to 0 or 1). The smaller the parameter, the faster, and more drastic, the increase in the internal resistance. Thus, the figure shows that the resistance increases faster as the SOC tends towards 1 (as $\beta_{2,w}$ is smaller than $\beta_{1,w}$) compared to the SOC tending towards 0. The $\boldsymbol{\beta}$ parameters together are used to control the minimum expected internal resistance (at an SOC of 0.5). This, as seen in Fig. 7, stayed fairly consistent across time. Thus, if $\beta_{1,w}$ and $\beta_{2,w}$ decrease over time resulting in an increased internal resistance, then $\beta_{0,w}$ has to decrease to keep the minimum expected internal resistance consistent.

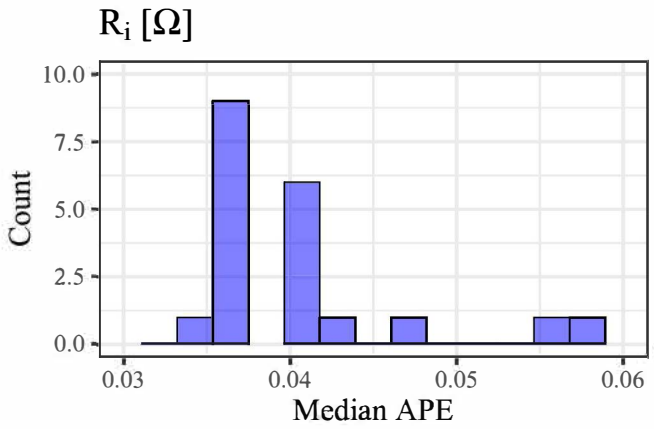

Fig. 9. Histogram of the median APE of every week, for resistances extracted when is required a period of relaxation at least as long as the previous current pulse.

B. Prediction of the battery age

Based on the model described in the previous section, the battery internal resistance can be accurately predicted, given a SOC value and the battery age (i.e., the week value). However, estimating the batterys age (i.e., week) knowing the resistance value and the SOC at which it was determined is also of interest; to be more precise, the probability distribution of $\mathbb{P}(w|R_i, \text{SOC})$ has to be determined. In order to evaluate this distribution, something has to be assumed about the probability distribution of the SOC, the week, and the joint distribution of resistance, SOC, and week. Starting with the joint distribution, by the definition of conditional probabilities [7] and under the assumption that the SOC and week are independent (which must be true), it can be written:

$$\mathbb{P}(\log(R_i), \text{SOC}, W) = \mathbb{P}(\log(R_i)|\text{SOC}, W)\mathbb{P}(\text{SOC})\mathbb{P}(W). \quad (5)$$

Thus, the joint distribution can be split into three parts, $\mathbb{P}(\log(R_i)|\text{SOC}, W)$, $\mathbb{P}(\text{SOC})$, and $\mathbb{P}(W)$. The conditional distribution of the internal resistance given the SOC and week, $\mathbb{P}(\log(R_i)|\text{SOC}, W)$, is the model described in the previous section. Furthermore, the marginal distributions of the SOC

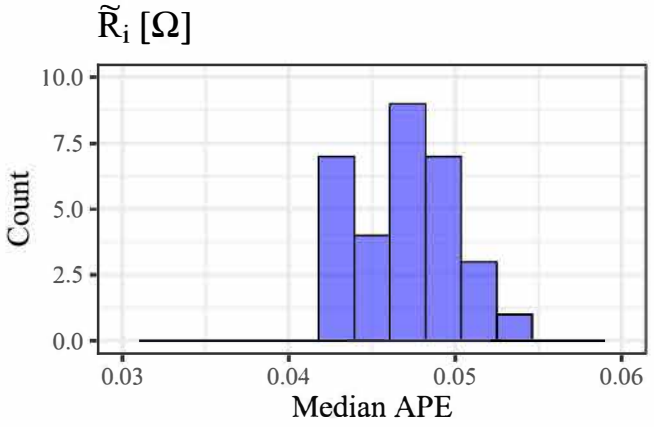

Fig. 10. Histogram of the median APE of every week, for resistances extracted where is required ony one second of relaxation before the current pulses.

and week, $\mathbb{P}(\text{SOC})$ and $\mathbb{P}(W)$, respectively, have to be defined. In this context, these distributions should be interpreted as a priori information. That is, if any prior information about the distribution of SOC or week are known, they should be considered at this point. However, in this paper, it will be assumed that any value of SOC and week is equally likely a priori. Consequently, it is assumed that the battery SOC follows a continuous uniform distribution on the unit interval and the week will follow a discrete uniform distribution over the set of possible weeks. Following this reasoning, the posterior distribution of the weeks, given the battery resistance and SOC can be calculated using:

$$\mathbb{P}(W|\log(R_i), \text{SOC}) = \frac{\mathbb{P}(\log(R_i)|\text{SOC}, W)\mathbb{P}(\text{SOC})\mathbb{P}(W)}{\sum_{w=1}^{\#\text{no. total weeks}} \mathbb{P}(\log(R_i)|\text{SOC}, w)\mathbb{P}(\text{SOC})\mathbb{P}(w)} \quad (6)$$

The posterior distribution (6) follows from the application of Bayes rule and the law of total probability to (5). The exact distribution of the battery cell week will be summarised by its weighted median and high posterior density region (HPD). A 95% HPD region represents the smallest possible combination of regions with a combined probability (area beneath the curve) of 95%.

Fig. 12 – Fig. 14 show the exact posterior probability of the week, given an internal resistance of 15 mΩ measured at SOCs of 20, 50, and 80%, respectively. These figures, in general, show a very consistent posterior probability across weeks, at around 2-4%. In particular, given a resistance of 15 mΩ, the posterior distributions at 20 and 80% SOC are almost identical, although we see that it is slightly more likely that the battery was 35 weeks (or older) if the resistance was measured at 20% SOC, than at 80% SOC. These sound like small probabilities, but looking at Fig. 7, we see that by drawing a line at 0.015 Ω on the ordinate axis, it would be almost exactly in the middle of all three confidence intervals. This can also be observed by the weighted median which ranged 17.4 – 24.7 weeks, and the 95% HPD regions, the blue shaded area of the figures, which stretches over the entire considered aging period (i.e., weeks 1 to 38) in all three figures – making the HPD useless for interpretation in this case. This is to be expected, as the battery's internal resistance only increased by 8.7% during the 38 weeks of aging, as seen in Fig. 3. Furthermore, the difference between the posterior distributions at 20 and 80% SOC should also be expected because the parameter $\beta_{2,w}$ decreases faster than $\beta_{1,w}$, as seen in Fig. 11.

Fig. 15 – Fig. 17 show the exact posterior probability of week, when the internal resistance was increased from 15 mΩ to 20 mΩ, and the SOC was kept at 20, 50, and 80%, respectively. Similar with an internal resistance of 15 mΩ, the posterior probability distributions at 20 and 80% SOC are almost identical. The HPD regions show that the batteries have a 95% probability of being older than 22.8 and 27.5 weeks given that the internal resistance of 20 mΩ was measured at 20% and 80% SOC, respectively. This is also seen from the blue shaded area in the corresponding figures. In both cases, the mode of the distribution (its highest point) is at 38 weeks with a probability larger than 0.2, and the weighted median week is around 35. This is also reflected in the posterior distribution at 50% SOC, with a mode at 38 weeks where the probability is slightly larger than 0.15. However, at 50% SOC we also see a higher probability around weeks 1-10, as seen from the 95% HPD which is the union of $[1; 12]$ and $[23; 38]$. This is caused by an initial decrease in the internal resistance, measured at around 50% SOC, during the first few weeks of aging. Furthermore, this phenomenon is magnified by the fact that the internal resistance does not increase as much at 50% SOC, when compared to 20% and 80% SOC – this is also seen by comparing the trajectories of the curves corresponding to each of the three SOC values, which can be seen in Fig. 3.

V. Conclusions

In this paper, a methodology was proposed for identifying the battery internal resistance and model its degradation behavior directly from a dynamic aging profile. The resistance was extracted by keeping careful track of the changes to the current profile and, then, calculating the resistance of any given point in time, using Ohm's law. The internal resistance was defined as the resistance extracted after 18 seconds of consistent charging, and further limited to resistances calculated following a period of relaxation at least as long as the previous current pulse. The extracted internal resistance for a given week, was then modelled as a log-linear function of SOC. The model fitted to the extracted internal resistance was extremely consistent with the internal resistance obtained by a traditional method, and could easily be incorporated into a framework for finding the posterior probability distribution of battery cell being w weeks old, given an internal resistance measured at a SOC value. The analysis showed that the extracted internal resistance was fairly stable across weeks in, and around,

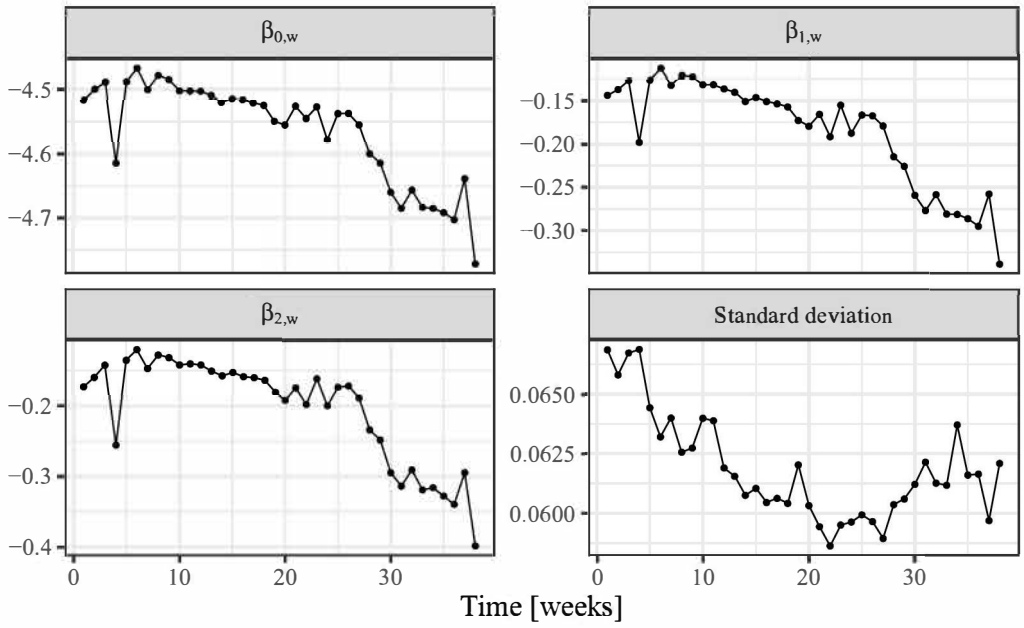

Fig. 11. The parameter estimates of the log-linear resistance model, given resistances extracted using a relaxation time larger to or equal to the length of the previous current pulse, for every week.

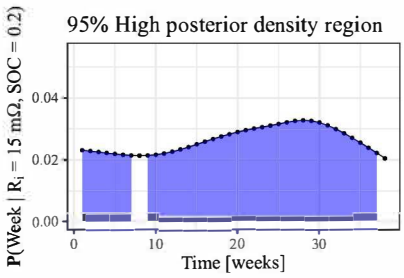

Fig. 12. The posterior distribution of the battery ageing week given a SOC of 20% and an internal resistance of 15 mΩ.

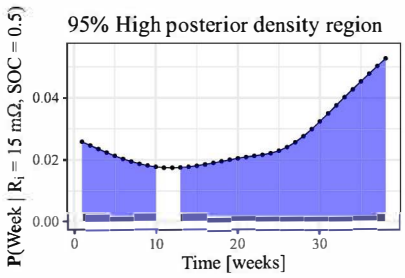

Fig. 13. The posterior distribution of the battery ageing week given a SOC of 50% and an internal resistance of 15 mΩ.

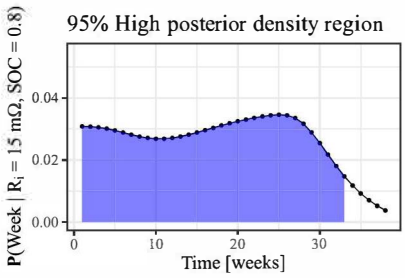

Fig. 14. The posterior distribution of the battery ageing week given a SOC of 80% and an internal resistance of 15 mΩ.

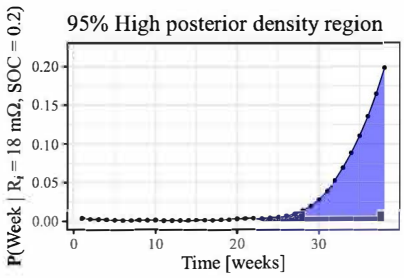

Fig. 15. The posterior distribution of the battery ageing week given a SOC of 20% and an internal resistance of 20 mΩ.

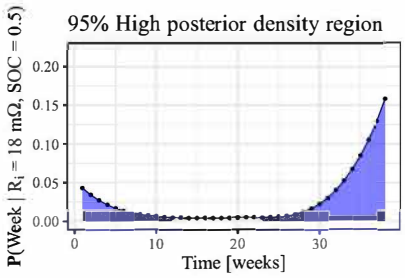

Fig. 16. The posterior distribution of the battery ageing week given a SOC of 50% and an internal resistance of 20 mΩ.

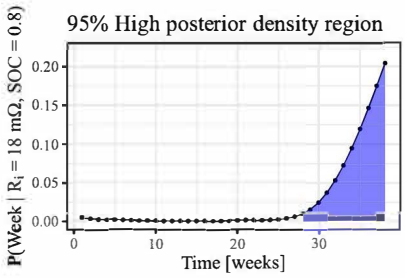

Fig. 17. The posterior distribution of the battery ageing week given a SOC of 80% and an internal resistance of 20 mΩ.

50% SOC, when compared to 20 and 80% SOC, where the internal resistance increased at a much higher rate. This was in complete concordance with the internal resistance obtained by traditional methods. Furthermore, this framework lends itself readily for an extension to estimating the battery's remaining useful life (RUL), as the posterior probability distribution of the week values can be directly translated to the RUL of the battery. However, this is left for future research. Lastly, another simple extension of the framework, not included in the present paper, is the learning of the SOC behavior, and how it relates to the use of the battery cell.

REFERENCES

[1] T. Reddy, Lindens Handbook of Batteries, 4th edition, McGraw Hill, 2010.

[2] Electrically propelled road vehicles – Test specification for lithium-ion traction battery packs and systems – Part 1: High-power applications, ISO 12405-1:2011.

[3] A.-I. Stroe, Analysis of Performance and Degradation for Lithium Titanate Oxide Batteries, PhD Thesis, Aalborg University, May 2018.

[4] N. Nieto et al., Thermal Modeling of Large Format Lithium-Ion Cells, Journal of The Electrochemical Society, vol. 160, no. 2, pp. A212-A217, 2013.

[5] D.-I. Stroe, M. Swierczynski, S.K. Kr, R. Teodorescu, Degradation Behavior of Lithium-Ion batteries during Calendar Ageing – The Case of the Internal Resistance Increase, IEEE Transactions on Industry Applications, vol. 54, no. 1, pp. 517-525, Jan.-Feb. 2018.

[6] H.-G. Schweiger et al., Comparison of Several Methods for Determining the Internal Resistance of Lithium Ion Cells, Sensors, vol. 10, no. 6, pp. 5604-5625, 2010.

[7] P. Olofsson and M. Andersson, Probability, statistics, and stochastic processes, 2nd edition, Wiley 2012.

[8] B.V· Ratnakumar, M.C. Smart, L. D., Whitcanack, R. C. Ewell, The impedance characteristics of Mars Exploration Rover Li-ion batteries, Journal of Power Sources, vol. 159, pp. 1428-1439, 2006.

[9] D.-I. Stroe, M. Swierczynski, S.K. Kr, E. Martinez-Laserna, and E. Sarasketa-Zabala, Accelerated Aging of Lithium-Ion Batteries based on Electric Vehicle Mission Profile, 2017 IEEE Energy Conversion Congress and Exposition (ECCE), Cincinnati, OH, 2017, pp. 5631-5637.

[10] T.R.B. Grandjean, J. Groenewald, A. McGordon, W.D. Widanage, J. Marco, Accelerated Internal Resistance Measurements of Lithium-Ion Cells to Support Future End-of-Life Strategies for Electric Vehicles, Batteries, vol. 49, no. 4, 2018.

[11] Y· Liu, Z. He, M. Gao, Y· Li, G. Liu, Dual Estimation of Lithium-ion Battery Internal Resistance and SOC Based on the UKF, 2012 5th International Congress on Image and Signal Processing, Chongqing, 2012, pp. 1639-1643.

[12] Y. Fang, R. Xiong, J. Wang, Estimation of Lithium-Ion Battery State of Charge for Electric Vehicles Based on Dual Extended Kalman Filter, Energy Procedia vol. 152, pp. 574-579, 2018

[13] A. Lievre, A. Sari, P. Venet, A. Hijazi, M. Ouattara-Brigaudet, S. Pelissier, Practical Online Estimation of Lithium-Ion BatteryApparent Series Resistance forMild Hybrid Vehicles, IEEE Transactions on Vehicular Technology, vol. 65, no. 6, pp. 4505-4511, June 2016.

[14] M. Ecker, N. Nieto, S. Kabitz, J. Schmalstieg, H. Blanke, A. Warnecke, D. U. Sauer, Calendar and cycle life study of Li(NiMnCo)O2-based 18650 lithium-ion batteries, Journal of Power Sources, vol. 248, pp. 839-851, February 2014.

[15] D.-I. Stroe, "Lifetime Models for Lithium-ion Batteries used in Virtual Power Plant Applications," PhD Thesis, Aalborg University, Nov. 2014.